ELABORATION AND CHARACTERIZATION OF A COMPLEX COATING ON Ti WITH TiO_2 NANOTUBES, FUNCTIONALIZED SINGLE CARBON NANOTUBES, HYDROXYAPATITE AND IRON

Luiza ICHIM[1], Cristina DUMITRIU[2], Alina SURUGIU[3], Georgeta TOTEA[4], Ioana DEMETRESCU[5*]

Abstract. *The aim of this work is elaboration and characterization of a complex coating on Ti with TiO_2 nanotubes, functionalized single carbon nanotubes, hydroxyapatite (HA) and iron (Fe). The single carbon nanotubes (SWCNTs) were functionalized with carboxyl groups (SWCNT-COOH) and TiO_2 nanotubes were elaborated by anodization. The complex hybrid material with iron immobilized was obtained by chronopotentiometric method. The electrodeposited HA/ SWCNT-COOH/Fe coatings were investigated for two different concentration of Fe as 0.01 and 0.025 M respectively. The coating structures were studied by X-Ray Diffraction. Surface analysis was completed with contact angles determination in order to establish the hydrophilic/hydrophobic balance. Electrochemical determinations were followed by potentiodynamic measurements conducted in Hank solution and by electrochemical impedance spectroscopy investigations(EIS). As biological hemolysis experimentes were performed, and no sign of evident toxic efect was observed.*

Keywords: TiO_2 nanotubes, SWCNTs, hydroxyapatite**,** electrochemical tests, hemolysis.

1. Introduction

One of the most important topic of 21 century is the bioimplant design in order to obtain materials with remarkable properties. Those can be used in bone and joint replacements, fixation devices or dental implants to make our life easier.

There are many types of materials used to manufacture implantable devices, each one of them having special purposes depending on their compsition. They can be

* corresponding author
[1]PhD student, University Politehnica of Bucharest, Faculty of Applied Chemistry and Materials Science, Department of General Chemistry, 1-7 Polizu Street, sector 1, Bucharest, 011061 (e-mail: necula_luiza@yahoo.com).
[2]PhD, University Politehnica of Bucharest, Faculty of Applied Chemistry and Materials Science, Department of General Chemistry, 1-7 Polizu, Sector 1, Bucharest, 011061 (e-mail: dumitriu.cristina.o@gmail.com).
[3] Dr. Md., Clinic CF2 Hospital, 63 Marasti, Sector 1, Bucharest, Romania (email: surugiualina@yahoo.com)
[4]PhD, Buftea M. Burghele Hospital, Studioului 5, Buftea, Romania (email:)
[5]Prof., PhD., University Politehnica of Bucharest, Faculty of Applied Chemistry and Materials Science, Department of General Chemistry, 1-7 Polizu, Sector 1, Bucharest, 011061 (e-mail: **ioana_demetrescu@yahoo.com**)

metallic biomaterials, polymers or ceramics materials. The main merit of these materials is high biocompatibility (non-toxic, non-allergic) with human tissue [2].

Magnesium, iron and zinc base materials have been studied for this purpose. Iron is an essential element for human body, and is used also for the transfer of oxygen by blood [3] and have many others applications, like catalysts for growing carbon nanotubes or photodecomposing organics [4].

Compared to magnesium porous structure, iron posses higher strenght which leads to a better control over the porous structure[5], and also have a better ductility and radio-opaqueness, than magnesium and it's alloys [6], but iron presents some problems due to it's ferromagnetic behaviour and slow degradation rate [7].

Iron oxide is used used as a consequence of it's superparamagnetic properties as contrast agent for diagnostic imaging and magnetic drug delivery [8,9].

Titanium is among the most used scaffold for bioimplant applications as a result of his good corrosion resistance and high strength to be used as load-bearing. An inexpensive method to improve Ti bioactivity represents the formation of Titanium oxide nanotubes via anodization method [10].

A simple way to improve the osseointegration is to cover the metallic implants (Ti) with Hydroxyapatite [11]. This is the major mineral component of human hard tissue, having the ratio of Ca/P of 1.67 which helps to enhance bone recovery and is distinguished by his excellent biocompatibility and low price [12,13].

The researchers tried to incorporate hydroxyapatite with different compounds e.g.: iron ions, carbon nanotubes, etc. in order to obtain materials with better mechanical properties.The iron ions incorporation into hydroxyapatite can be obtained via sol-gel method [14], wet precipitation method [15], or by using the wet chemical method [16]. Gamal et al. demonstrated that the presence of iron addtives in HA structure is leading to the appearance of the point defects obtaining a new hard, strong and durable material.

K.M.T. Ereiba et al. developed FeHAp samples through wet chemical methods and established that iron improved the bio- activity and solubility of HAp under the physiological conditions [17].

The surfaces changes and immobilization of different biomolecules [18] [19], ions [20], nanoparticles [21], nanotubes [22] on biomaterials surface has been applied to improve the biocompatibility of implants. The biological response of biomaterial has a close relationship with the interaction between cells and surfaces.

Platelet adhesion and endothelialization rates are frequently used to assess the biocompatibility of biomaterials [23]. Plateletes are disc shaped blood cells emitting pseudopodia when activated in certain conditions .

Red blood cells can be affected also, the interaction between erythrocytes and the materials may lead to certain changes in cell surface features, even more some materials have hemolytic action on normal human erythrocytes in vitro.

Many attempts appear in literature regarding CNTs reinforced Hydroxiapatite as CNTs have caught the attention in medical field due to to their unique structure, high surface area, electrical conductivity and low weight [24]. These nanocomposites can be used for bone replacements and could be developed via ion exchange reaction or sol-gel process [25] .

The present paper aims to obtain by chronopotentiometric method a coating material based on TiO_2 nanotubes, hydroxyapatite, iron ions and functionalized single wall carbon nanotubes with carboxyl groups (SWCNT-COOH). We proposed to establish the SWCNTs-COOH influence from electrochemical study in Hank solution and also their biological performance. In our previous work [26] 2 materials containing TiO_2 nanotubes, hydroxyapatite and iron ions with two diferent concentration (0.01M and 0.025M) were developed. Analyses of the iron behaviour via electrochemical study in Hank solution showed that the increase of iron concentration lead to a higher corrosion rate. We compared the biological behaviour of the new materials with our 2 samples previously developed (TiO2-HA-Fe 0.01 , TiO2-HA-Fe 0.025).

2. Materials and methods

2.1. Functionalization of SWCNTs with –COOH groups

SWCNTs functionalization [27] is necessary in order to introduce -COOH groups . SWCNTs are from Sigma Aldrich and have diameter between 20-40 nm and length from to 10μm.

The functionalization was performed using aqua regia 2:3 (V:V), 8 h at 50 degree. After this step the samples were washed with ultrapure water and dried.

2.2 Anodization of Ti plates

The titanium sample (99.7% purity, 2mm thick, Sigma-Aldrich) has a selected area of 0.385 cm^2 . The electrochemical anodizing of titanium samples was performed in order to obtain TiO_2 nanoarhitectures . We used an electrochemical cell with 2 electrodes, with Platinum sheet as a counter electrode, the voltage was kept constant at 20 V, for 1.5 h at room temperature. Anodizing was carried out using HF 0.5% and Na_2HPO_4 5g/L electrolyte. [26].

2.3. Electrodeposition of HA/ SWCNT-COOH/Fe hybrid material

The electrochemical cell was consisted from anodic titanium nanotubes obtained above, a platinum counter-electrode and with Ag/AgCl as a reference by chronopotentiometric method for 30 minutes. The electrolyte had the following composition: 2 g/L SWCNT-COOH, 9.91 g/L $Ca(NO_3)_2 \cdot 4H_2O$, and 2.875 g/L $NH_4H_2PO_4$. We used two different concentration of $Fe(NO_3)_3$ $9H_2O$ 0.01M and 0.025 M, which was added into the solution mentioned above.

We will refer to 4 samples: sample 1 - TiO2HA-Fe 0.01 electrodeposition of HA-Fe 0.01M on TiO_2 nanotubes obtained by anodization on titanium, sample 2 - TiO2HA-Fe 0.025 electrodeposition of HA-Fe 0.025M on TiO_2 nanotubes obtained by anodization on titanium, sample 3 - TiO2HA-Fe-Swcnt 0.01M electrodeposition of HA- Fe 0.01M and SWCNTs-COOH on TiO_2 nanotubes obtained by anodization on titanium, sample 4 - TiO2HA-Fe-Swcnt 0.025 M electrodeposition of HA-Fe 0.025M and SWCNTs-COOH on TiO_2 nanotubes obtained by anodization on titanium.

2.4. Surface characterization

In order to examine the formation of HA layer also the presence of iron and SWCNTs-COOH we used the bellow methods:

2.4.1. X-Ray Diffraction (XRD)

We used X-ray diffraction (XRD) in order to determine the dimensional parameters of crystals

2.4.2. Static contact angle

Surfaces can be characterized as being hydrophilic or hydrophobic depending on the value of the contact angle. An angle value less than 90 ° means that the surface has a hydrophilic behaviour; while an angle above 90 ° characterize a hydrophobic surface.

2.5. Biological test

We used the blood smear to examine the blood cells (leuckocytes, eritrocites and platelets) for any modification in size and shape according to known standards [28, 29]. We have chosen fresh blood from a healthy pacient on EDTA vacuum tubes, having normal hemoleucograme parameters that can be seen in table 1, obtained by couning with an automatic hematology analizer type Sismex.

Table 1. Hemoleucograme parameters

Parameter	*Result*	*Reference values*
WBC (LEUCOCITE)	7.35 [10^3/uL]	4.00 - 11.00
RBC(ERITROCITE)	5.01 [10^6/uL]	4.00 - 6.30
HGB(HEMOGLOBINA)	13.8 [g/dL]	12.00 - 18.00
HCT(HEMATOCRIT)	41.2 [%]	37.00 - 51.00
MCV	82.2 [fL]	80.00 - 97.00
MCH	27.5 [pg]	26.00 - 32.00)
MCHC	33.5 [g/dL]	31.00 - 36.00
PLT (TROMBOCITE)	204 [10^3/uL]	140-440)
NEUT%	79.0 [%]	37.00 - 92.0
LYMPH%	15.1[%]	10.00 - 58.0
MONO%	4.4 [%]	0.0 - 14.0
EO%	1.2 [%]	0.0 - 6.0
BASO%	0.3 [%]	0.0 - 1.0

The materials were placed in Petri dishes in humid environment in order to avoid blood dehydration, then 200 microliters blood was added on the materials surface.

The Petri dishes were incubated for 30 minutes, respectively 60 minutes at 37°C. The smears were prepared using 5 microliters of blood from the fresh blood and at each interval from all samples. The smears were colored using May-Grumwald-Giemsa method using reagents from Merck, and the immersion reading was made with an optical microscope.

2.6. Electrodeposition of HA/ SWCNT-COOH/Fe hybrid material

The electro-deposition resulted curves are presented in Fig. 1. It can be seen that they are similar to the ones reported in the literature by having the signal divided into 3 time sections. As expected, we obtained the same results as previously mentioned in the literature [11]. Further the hybrid ceramic material structure was studied by X-Ray Diffraction.

3. Results and discussion

3.1. X-Ray Diffraction (XRD)

The samples were analysed with D8 DISCOVER, Bruker diffractometer equipped with Gobell mirror, LynxEye 0D detector and Cu tube. We used the below measuring conditions: 0.040 increment, the scanning speed was 3s / pas and theta tangential incidence of 10. Measuring range was between 200 - 800.

Based on the qualitative analysis phase we identified the compounds with Ti, Fe, C, Ca, O, standing out C (Swcnts), TiO_2, $Fe(OH)_2$, $CaFe_2O_4$, $Fe_2Ti_3O_9$ structures.

For both our samples, the C (Swcnts) compound have a hexagonal structure and this appears at 2θ = 250, 430 and 530, being better shaped for TiO2HA-Fe-Swcnt 0.01M sample (Table 2, Fig. 2).

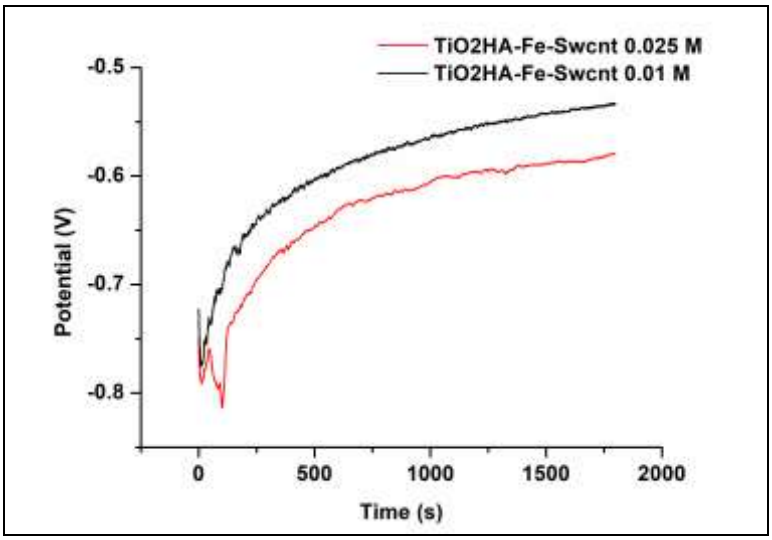

Fig. 1. The electrodeposition curve for HA onto TiO_2 on titanium plates

Table 2. Crystallite average size calculation and elementary cell parameters for TiO2HA-Fe-Swcnt 0.01M and TiO2HA-Fe-Swcnt 0.025M samples

Compounds	*Crystallographic phase*	*Crystallite average size*	*Crystallization system*	*Elementary cell parameters*
TiO2HA-Fe-Swcnt 0.01M	$Ti_{0.325}$	D = 178.4 Å	Hexagonal	a = 2.9700; c = 4.7751
	$Fe_{0.96}(OH)$	D = 181.6 Å	Hexagonal	a = 2.9630 ; c = 9.3700
	C	D = 461.8 Å	Hexagonal	a = 2.4285; c = 6.9279
TiO2HA-Fe-Swcnt 0.025M	Ti	D = 206.8 Å	Hexagonal	a = 2.9700; c = 4.7200
	Fe_4N	D = 353.9 Å	Cubic	a = b = c = 3.3800
	$Fe_2Ti_3O_9$	D = 340.3 Å	Hexagonal	a = 2.8667; c = 4.5985

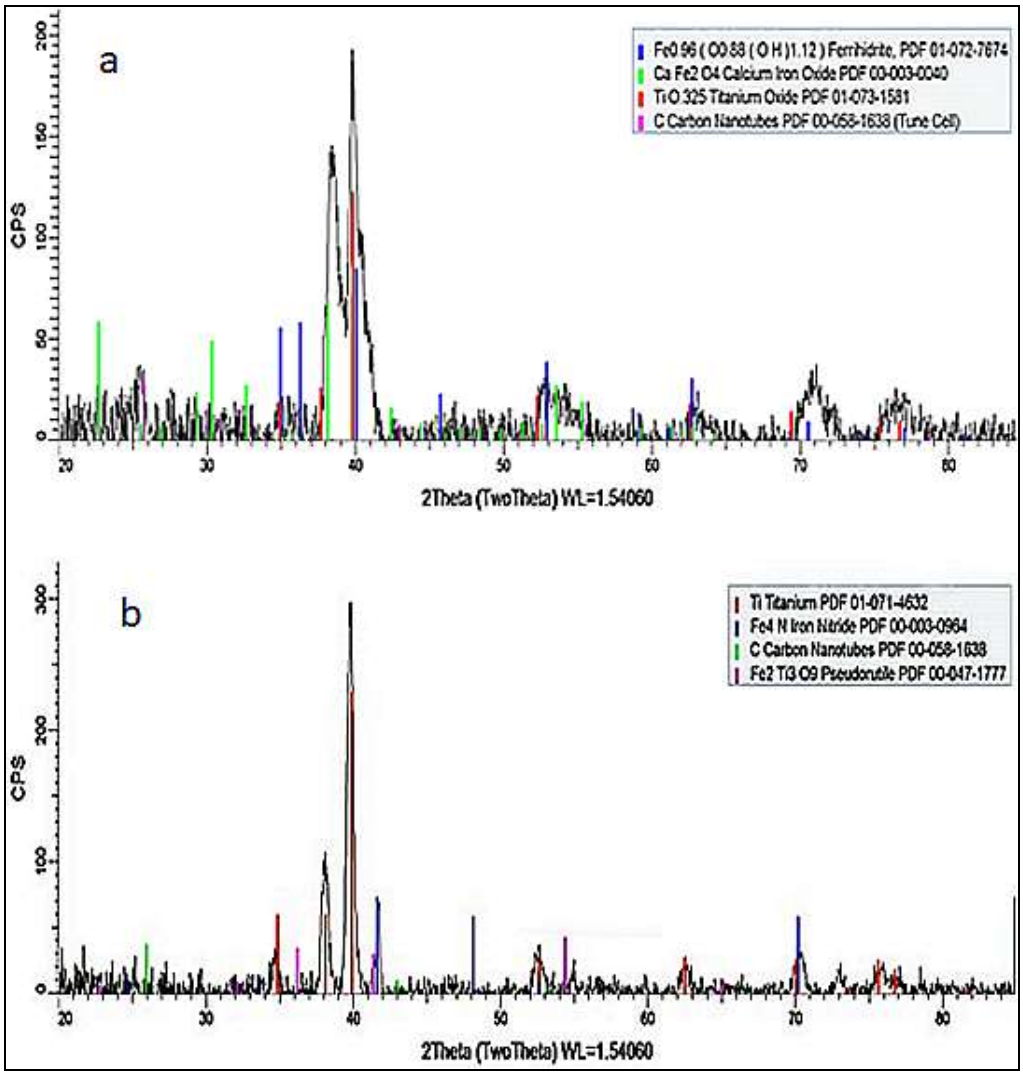

Fig. 2. XRD pattern for: a) TiO2HA-Fe-Swcnt 0.01M and b) TiO2HA-Fe-Swcnt 0.025 M

3.2. Static contact angle

We performed the wettability studies in order to characterise the nature of the surface. The contact angle measurements were performed at room temperature. The tests were performed with distilled water. The obtained results for both samples are represented in Table 3. In this case the recorded values show a strong hydrophilic character.

Table 3. Contact angle values for TiO2HA-Fe-Swcnt 0.01 M and TiO2HA-Fe-Swcnt 0.025 M samples

Materials	***Contact angle***	***STDEV %***
TIO2HA-Fe-Swcnt 0.01 M	21.48	1.4
TIO2HA-Fe-Swcnt 0.025 M	27,38	1.9

3.3. Electrochemical behaviour

The EIS measurement were performed at open circuit potential and were presented in Bode plots in Fig. 3a and Fig. 3b.

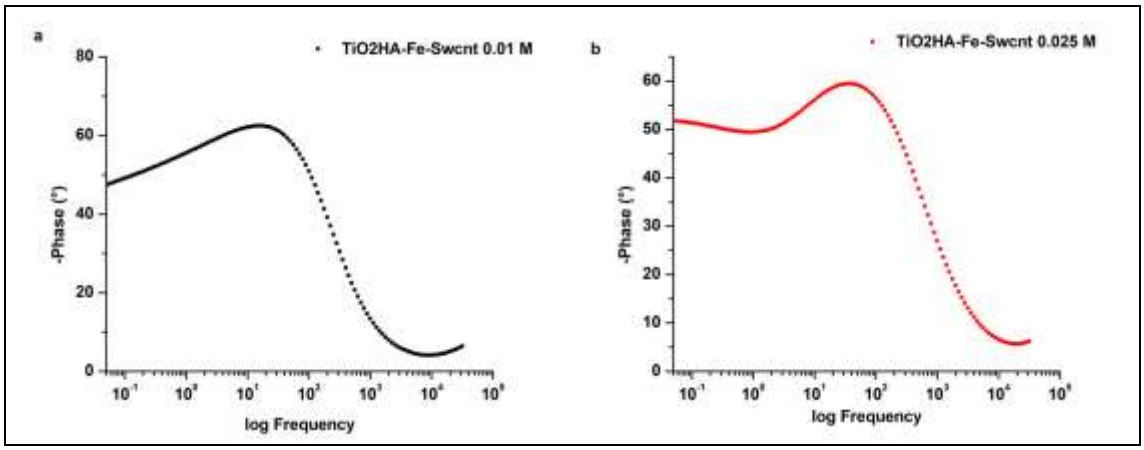

Fig. 3. Bode plots for: a) TiO2HA-Fe-Swcnt 0.01 M sample and b) TiO2HA-Fe-Swcnt 0.025 M sample in Hank solution

Both materials TiO2HA-Fe-Swcnt 0.01 M and TiO2HA-Fe-Swcnt 0.025 M have the phase angle at 50 degree for low frequencies and increase to medium frequencies at 60 degrees, having a diffusive behavior with capacitive tendency. It can be seen that the phase angle for high frequencies is decreasing. The materials have the same behavior as TiO2HA-Fe-0.025 material.

Electrochemical study was followed by potentiodynamic measurements conducted in Hank solution presented in Fig. 4.

From Table 4 we can notice that the corrosion rates for both sample is in domain of perfect stable values. The EIS obtained dates were fitted with Nova 1.7 software, obtaining the circuit from Fig. 5.

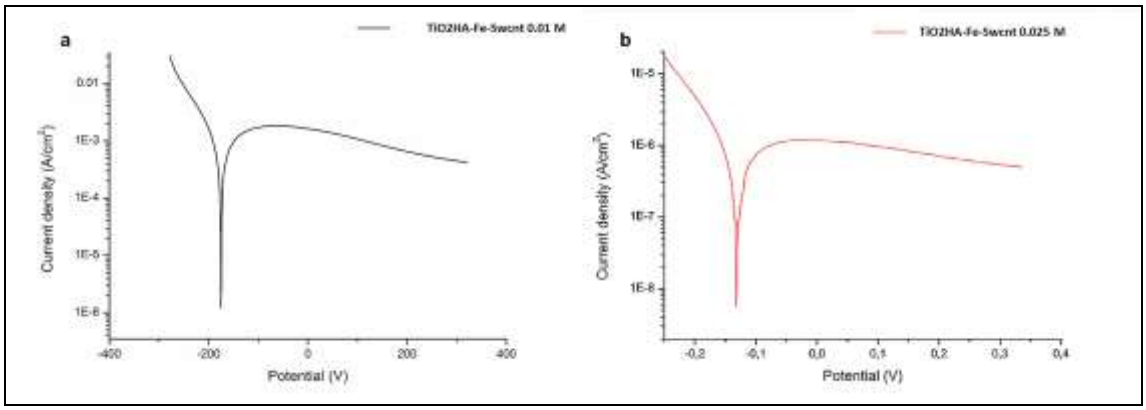

Fig. 4. Polarization curve for: a) TiO2HA-Fe-Swcnt 0.01 M sample and b) TiO2HA-Fe-Swcnt 0.025 M sample in Hank solution

Table 4. Corrosion parameters from Tafel polarization curves obtained for TiO_2HA-Fe-SWCNTs 0.01 and TiO_2HA-Fe-SWCNTs 0.025 samples in Hank solution

Sample	***E_{cor}, (V)***	***j_{corr} (A/cm²)***	***i_{cor}, (A)***	***Corrosion rate, (mm/year)***	***Polarization resistance (Ω)***
TIO2HA-Fe-Swcnt 0.01 M	- 0.17433	$6.1162*10^{-7}$	$6.9174E*10^{-7}$	0.0053225	29835
TIO2HA-Fe-Swcnt 0.025 M	- 0.13162	$6.0431*10^{-7}$	$6.8348E*10^{-7}$	0.005259	39244

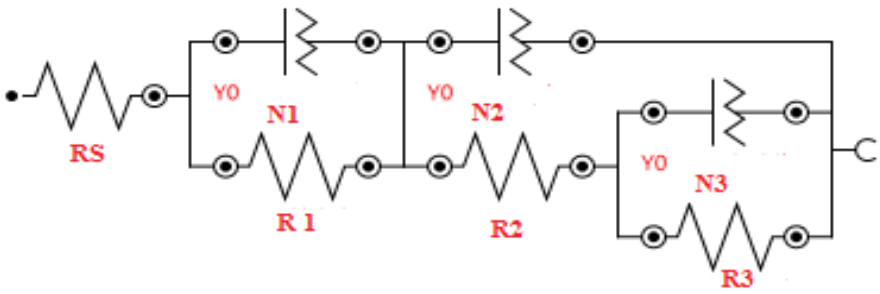

Fig. 5. The circuits for EIS data fit for TiO2HA-Fe-Swcnt 0.01 M and TiO2HA-Fe-Swcnt 0.025 M samples

Rs is the solution resistance, R1 the resistance of barrier layer, R2 is the resistance of the porous layer, R3 is the polarization resistance of the apatite layer. The obtained parameters are shown in Table 5.

Table 5. The fitting values obtained from the equivalent circuit for TIO2HA-Fe-SWCNTs-0.01, TIO2HA-Fe-SWCNTs-0.025 samples in Hank solution.

Material	*Rs (Ω)*	*R_1 (Ω)*	*n_1*	*R_2 (Ω)*	*n_2*	*R_3 (Ω)*	*n_3*
TiO2HA-Fe-Swcnt 0.01 M	9.08	50.5	0.815	918	0.888	$515x10^3$	0.49
TiO2HA-Fe-Swcnt 0.025 M	9.01	46.2	0.996	317*10	0.8	$144x10^4$	0.572

3.4. Biological analysis

First two images (Fig. 6) present the first smear used as control, in order to observe the structure and shape of the normal cells before having contact with the materials. In the fig. 6 a are highlighted three neutrophyles, two platelets and normal erythrocytes, in 6 b a monocyte, a platelet and some red blood cells. As can be seen, the membrane of the RBC are neet, smooth edges, and one third of the cells are empty. So, the blood chosen for testing is normal, the erythrocyte, leukocyte and platelet series are normal it is to mention that some authors have correlated the blood-contacting behaviour of surfaces with their interfacial free energy and surface chemistry [30].

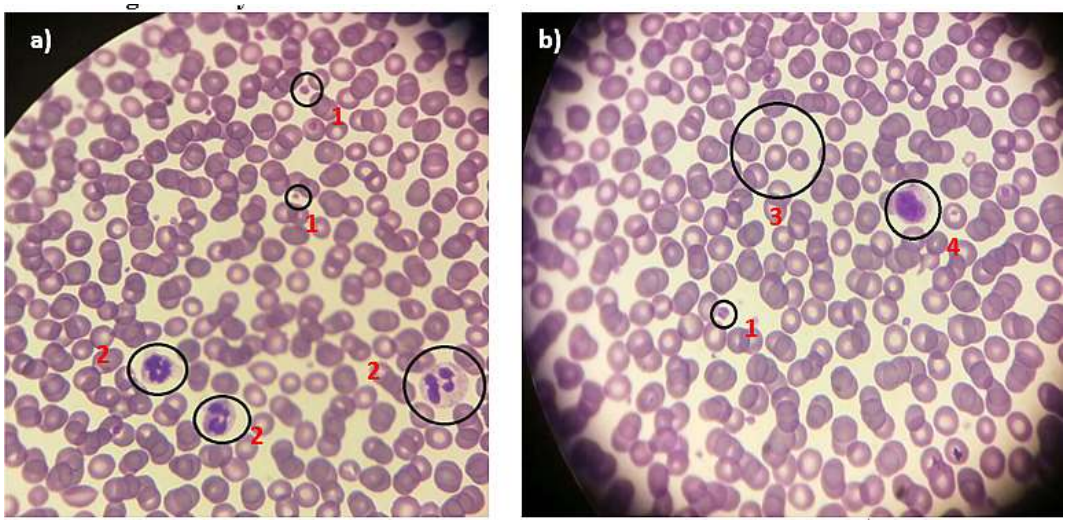

Fig. 6. The control smear (1-platelets, 2-neutrophiles, 3-red blood cells, 4-monocyte)

For TiO2HA-Fe 0.01 sample we can observe after 30 minutes (Fig. 7 a, b, c) that the lymphocyte and neutrophiles did not change the shape, but the trombocites start to change, they developed pseudopodes, in order to be able to adhere to the material. After one hour (Fig. 7 d, e, f), also no changes in RBC, neutrophyles and lymphocytes, the trombocytes have pseudopodes.

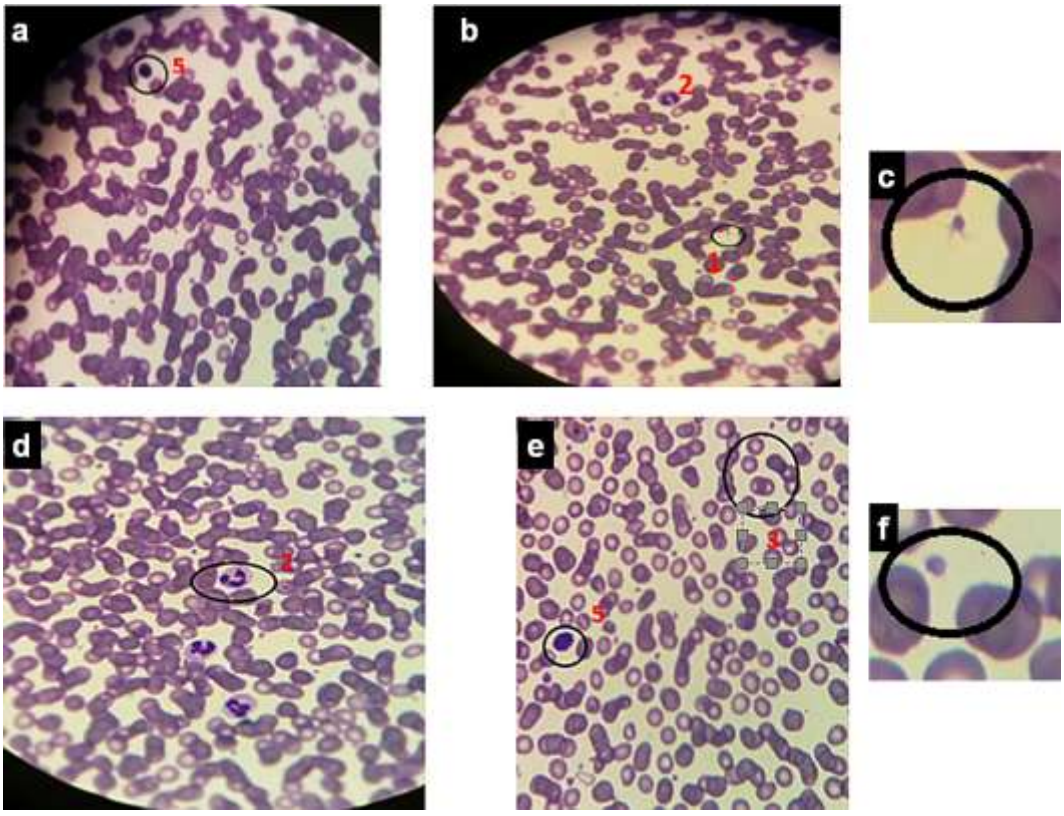

Fig. 7. TiO2HA-Fe 0.01 sample
30 minutes with: a) normal lymphocyte (5), b) with normal neutrophiles (2) an platelets with pseudopodes (1), c) platelet with pseudopodes; and 60 minutes with: d) normal neutrophiles (2), e) normal lymphocyte (5), red blood cells (3) f) platelet with pseudopodes

For sample TiO2HA-Fe 0.025 (Fig. 8) can be observed the same type of behavior like sample TiO2HA-Fe 0.01 sample, for both 30 and 60 minutes, no modification in blood cells shape, except pseudopodes in trombocytes.

For TiO2HA-Fe-Swcnt 0.01 M sample (Fig. 9 a) and TiO2HA-Fe-Swcnt 0.025 M sample (Fig. 10 a) in the first 30 minutes nothing happened, but after 60 minutes (Fig. 9 b and 10 b) we observe the apparition of echinocytes, red blood cels with scalloped edges, due to a slight degradation of RBC in contact with the material. Pseudopodes in trombocytes are prezent, so they adhere to the material.

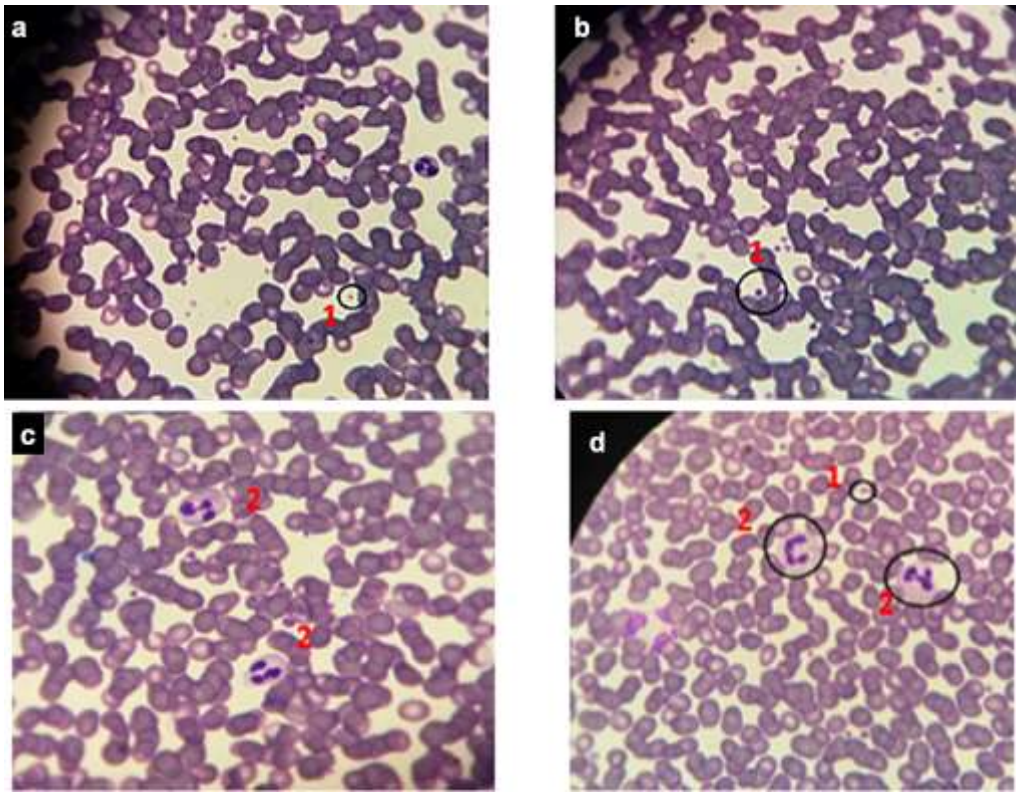

Fig. 8. TiO2HA-Fe 0.025 sample
30 minutes with: a) neutrophyles and platelets, b) platelets;
and 60 minutes with: c) normal neutrophyles, d) trombocytes having pseudopodes

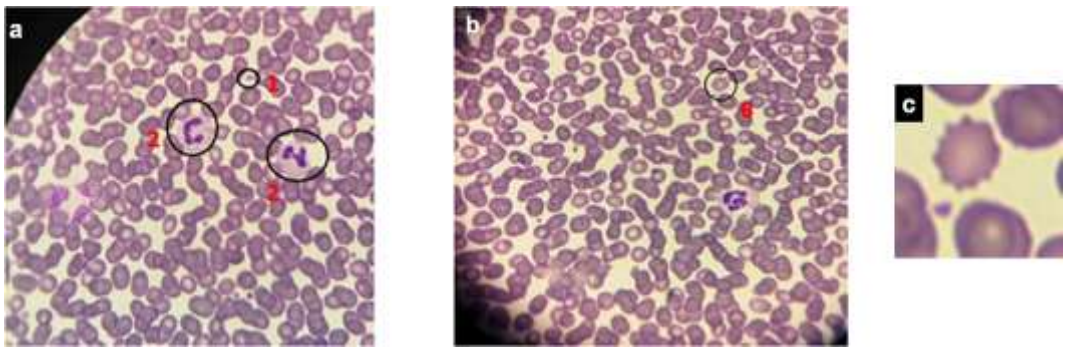

Fig. 9. TiO2HA-Fe-Swcnt 0.01 M: a) 30 minutes (normal elements), b) 60 minutes (6-echinocyte) and c) echinocytes

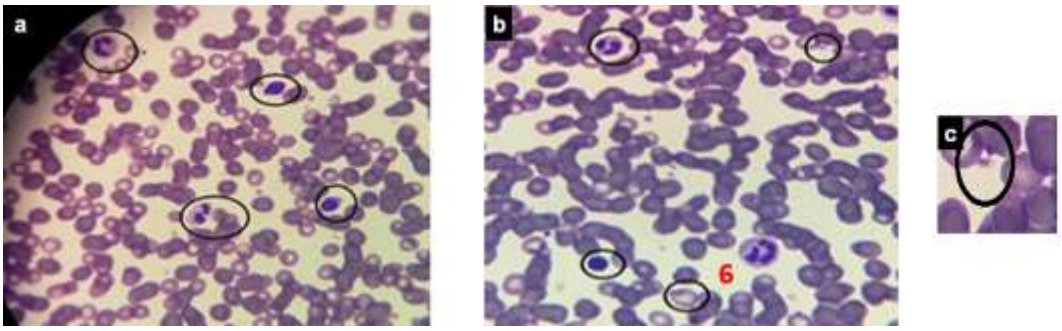

Fig. 10. TiO2HA-Fe-Swcnt 0.025 M: a) 30minutes, b) 60minutes (6-echinocytes) and c) Trombocytes with pseudopodes

Conclusions

In this study we investigated the corrosion behaviour of a new composite TiO2 HA-Fe-Swcnt 0.025 M material versus TiO2HA-Fe-Swcnt 0.01 M.

The contact angles measurements for both investigated samples, reveales a strong hydrophilic behavior.

The samples structure was investigated via XRD analysis and we obtained a hexagonal structure for the C (SWCNTs) compound from both our samples. The corrosion rate values for all coatings immersed in Hank solution at 37 °C are in the perfect stable domain of corrosion resistance.

After biological tests we can notice no sign of evident toxic efect was observed, meaning no signs of hemolysis were observed in all samples, only a slight degradation of RBC after one hour of contact and also, no tendency to forming agregates in case of platelets was observed. The pseudopodes were produced in all samples very quickly, even after 30 minutes.

REFERENCES

1. Peuster M., Wohlsein P., Brügmann M., Ehlerding M., Seidler K., Fink C., Brauer H., Fischer A., Hausdorf G., (2001) A novel approach to temporary stenting: degradable cardiovascular stents produced from corrodible metal—results 6–18 months after implantation into New Zealand white rabbits, Heart, 86, 563–569.

2. Farack J., Wolf-Brandstetter C., Glorius S., Nies B., Standke G., Quadbeck P., Worch H., Scharnweber D., (2011), The effect of perfusion culture on proliferation and differentiation of human mesenchymal stem cells on biocorrodible bone replacement material, Materials Science and Engineering B 176, 1767–1772.

3. Vojtech D., Kubasek J., Capek J., Pospisilova I., (2015), Comparative mechanical and corrosion studies on magnesium, zinc and iron alloys as biodegradable metals, Materials and technology, 49, 877–882.

4. Gan Y. X., Gan B. J., Zhang L., (2011), Electrochemical deposition of iron nanoneedles on titanium oxide nanotubes, Materials Letters, 65, 2992–2994.

5. Daud N. M., Sing N. B., Yusop A. H., Majid F. A. A., Hermawan H., (2014), Degradation and in vitro cellematerial interaction studies on hydroxyapatitecoated biodegradable porous iron for hard tissue scaffolds, Journal of Orthopaedic Translation, 2, 177-184.

6. Francis A., Yang Y., Virtanen S., Boccaccini A. R., (2015), Iron and iron-based alloys for temporary cardiovascular applications, Journal of Material Science Materials in Medicine , 26, 138-153.

7. Oriňaková1 R., Oriňak A., Kupková M., Hrubovčáková M., Škantárová L., Turoňová A. M., Bučková L. M., Muhmann C., Arlinghaus H. F., (2015), Study of electrochemical deposition and degradation of hydroxyapatite coated iron biomaterials, International Journal Electrochemical Science, 10, 659 – 670.

8. Panseri S., Cunha C., D'Alessandro T., Sandri M., Giavaresi G., M. Marcacci, Hung C. T., Tampieri A., (2012), Intrinsically superparamagnetic Fe-hydroxyapatite nanoparticles positively influence osteoblast-like cell behaviour, Journal of Nanobiotechnology, 10, 32-39.

9. Tran N., Mir A., Mallik D., Sinha A., Nayar S., Webster T. J., (2010) Bactericidal effect of iron oxide nanoparticles on Staphylococcus aureus, International Journal of Nanomedicine, 5, 277–283.

10. Portan D., Ionita D., Demetrescu I., (2009), Monitoring TiO2 nanotubes elaboration condition, a way for obtaining various characteristics of nanostructures, Key Engineering Materials, 415, 9-12.

11. Prodana M., Duta M., Ionita D., Bojin D., Stan M. S., Dinischiotu A. Demetrescu I., (2015), A new complex ceramic coating with carbon nanotubes, hydroxyapatite and TiO2 nanotubes on Ti surface for biomedical applications, Ceramics International, 41, 6318-6325.

12. Oriňaková R., Oriňak A., Kupková M., Hrubovčáková M., Markušová-Bučková L., Giretová M., Medvecký Ľ., Dobročka E., Petruš O., Kaľavský F., (2015), In Vitro Degradation and Cytotoxicity Evaluation of Iron Biomaterials with Hydroxyapatite Film, International Journal Electrochemical Science, 10, 8158 – 8174.

13. Chitsazi M. T., Shirmohammadi A., Faramarzie M., Pourabbas R., Rostamzadeh An., (2011), A clinical comparison of nano-crystalline hydroxyapatite (Ostim) and autogenous bone graft in the treatment of periodontal intrabony defects, Medicina Oral Patologia Oral Cirurgia Bucal, 16, 3, e448-453.

14. Mirestean C., Mocuta H., Turcu R. V. F., Borodi G. , Simon S., (2007), Nanostructurated materials for hyperthermia treatment of bonetumors", Journal of Optoelectronics and Advanced Materials, 9, 3, 764-767.

15. Peng F., Veilleux E., Schmidt M., Wei M., (2012), Synthesis of hydroxyapatite nanoparticles with tailorable morphologies and carbonate substitutions using a wet precipitation method, Journal of Nanoscience and Nanotechnology, 12, 3, 2774-2778,

16. Gamal G. A., Al-Mufadi F. A., Said A. H., (2013), Effect of Iron Additives on the Microstructure of Hydroxyapatite, ETASR - Engineering, Technology & Applied Science Research, 3, 6, 532-539.

17. Ereibia K. M. T., Mostafa A. G., Gamal G. A., Said A. H., (2013), In vitro study of iron doped hydroxyapatite, Journal of Biophysical Chemistry, 4, 4, 122-130.

18. Wise S. G., Michael P. L., Waterhouse A., Santos M., Filipe E., Hung J., Kondyurin A., Bilek M. M. M., Ng M. K. C., (2015), Immobilization of bioactive plasmin reduces the thrombogenicity of metal surfaces, Colloids and Surfaces B: Biointerfaces, 136, 944-954.

19. Gong F. R., Cheng X. Y., Wang S. F., Zhao Y. C., Gao Y., Cai H. B., (2010), Heparin-immobilized polymers as non-inflammatory and non-thrombogenic coating materials for arsenic trioxide eluting stents, Acta Biomaterialia, 6, 534-e546,

20. Sunarso Toita R., Tsuru K., Ishikawa K., (2016), Immobilization of calcium and phosphate ions improves the osteoconductivity of titanium implants, Materials Science and Engineering: C, 68, 291-298.

21. Heo D. N., Ko W.-K., Lee H. R., Lee S. J. , D. Lee, Um S. H., Lee J. H., Woo Y.-H., Zhang L. G., Lee D. W., Kwon K., (2016), Titanium dental implants surface-immobilized with gold nanoparticles as osteoinductive agents for rapid osseointegration, Journal of Colloid and Interface Science, 469, 129-137.

22. Zhang W., Jin Y., Qian S., Li J., Chang Q., Ye D., Pan H., Zhang M., Cao H., Liu X., Jiang X., 2014, Vacuum extraction enhances rhPDGF-BB immobilization on nanotubes to improve implant osseointegration in

ovariectomized rats, Nanomedicine: Nanotechnology, Biology and Medicine, 10, 8, 809-1818.

23. Li G., Yang P., Huang N., Ding H., (2013), Responses of platelets and endothelial cells to heparin/fibronectin complex on titanium: In situ investigation by quartz crystal microbalance with dissipation and immunochemistry, Journal of Bioscience and Bioengineering, 116, 235-245.

24. Shin U. S., Yoon I.-K., Lee G.-S., Jang W.-C., Knowles J. C., Kim H.-W., (2011), Carbon Nanotubes in Nanocomposites and Hybrids with Hydroxyapatite for Bone Replacements, Journal of Tissue Engineering, 2011, 674287, 10 pages;

25. Rajesh R., Senthilkumar N., Hariharasubramanian A., Ravichandran Y. D., (2012), Review on hydroxyapatite-carbon nanotube composites and some of their applications, International Journal of Pharmacy and Pharmaceutical Sciences, 4, 5, 23-27.

26. Ichim L., Sbarcea B. G., Patroi D., Dumitriu C., (2016), Hybrid bionic coating on Ti with TiO2 nanotubes, hydroxyapatite and iron, Revista de Chimie, 67, 11, 2198-2201.

27 Caoduro C., Hervouet E., Girard-Thernier C., Gharbi T., Boulahdour H., Delage-Mourroux R., Pudlo M., (2017), Carbon nanotubes as gene carriers: Focus on internalization pathways related to functionalization and properties, Acta Biomaterialia, 49, 36-44.

28 ISO 10993-4:2002/Amd 1:2006 Biological evaluation of medical devices Part 4: Selection of tests for interactions with blood, International Organization for Standardization, Geneva, Switzerland, 2009.

29 ASTM F756–00, Standard Practice for Assessment of Hemolytic Properties of Material, ASTM International, West Conshohocken, PA, USA, 2004.

30. Hunt B. J., Paratt R., Cable M., Finch D., Yacoub M., (1997), Haemocompatibility evaluation of DLC- and SIC-coated surfaces, Blood Coagulation and Fibrinolysis, 8, 223-231.